Conserv Genet
DOI 10.1007/s10592-007-9482-0

RESEARCH ARTICLE

Molecular and phenotypic diversity in *Chionactis occipitalis* (Western Shovel-nosed Snake), with emphasis on the status of *C. o. klauberi* (Tucson Shovel-nosed Snake).

Dustin A. Wood · J. M. Meik · A. T. Holycross · R. N. Fisher · A. G. Vandergast

Received: 21 August 2007 / Accepted: 5 December 2007

Abstract *Chionactis occipitalis* (Western Shovel-nosed Snake) is a small colubrid snake inhabiting the arid regions of the Mojave, Sonoran, and Colorado deserts. Morphological assessments of taxonomy currently recognize four subspecies. However, these taxonomic proposals were largely based on weak morphological differentiation and inadequate geographic sampling. Our goal was to explore evolutionary relationships and boundaries among subspecies of *C. occipitalis*, with particular focus on individuals within the known range of *C. o. klauberi* (Tucson Shovel-nosed snake). Population sizes and range for *C. o. klauberi* have declined over the last 25 years due to habitat alteration and loss prompting a petition to list this subspecies as endangered. We examined the phylogeography, population structure, and subspecific taxonomy of *C. occipitalis* across its geographic range with genetic analysis of 1100 bases of mitochondrial DNA sequence and reanalysis of 14 morphological characters from 1543 museum specimens. We estimated the species gene phylogeny from 81 snakes using Bayesian inference and explored possible factors influencing genetic variation using landscape genetic analyses. Phylogenetic and population genetic analyses reveal genetic isolation and independent evolutionary trajectories for two primary clades. Our data indicate that diversification between these clades has developed as a result of both historical vicariance and environmental isolating mechanisms. Thus these two clades likely comprise 'evolutionary significant units' (ESUs). Neither molecular nor morphological data are concordant with the traditional *C. occipitalis* subspecies taxonomy. Mitochondrial sequences suggest specimens recognized as *C. o. klauberi* are embedded in a larger geographic clade whose range has expanded from western Arizona populations, and these data are concordant with clinal longitudinal variation in morphology.

Keywords *Chionactis occipitalis* · mtDNA · Sonoran desert · Mojave Desert · ESU · Spatial genetic analysis

D. A. Wood (✉) · R. N. Fisher · A. G. Vandergast
U.S. Geological Survey, Western Ecological Research Center, San Diego Field Station, 4165 Spruance Road, Suite 200, San Diego, CA 92101, USA
e-mail: dawood@usgs.gov

J. M. Meik
Department of Biology, University of Texas at Arlington, Arlington, TX 76019, USA

A. T. Holycross
School of Life Sciences, Arizona State University, College and University Streets, Tempe, AZ 85287, USA

Introduction

The geographic distribution of genetic variation within species can provide valuable information on evolutionary and ecological processes, such as gene flow (migration and successful mating) and vicariance, which have shaped genetic diversity throughout species' history (Avise 1994; Templeton 1998). Gathering this information can also inform conservation decisions because effective management efforts often first require that distinct population segments or evolutionarily significant units are defined, often based on genetic and/or morphological patterns (USFWS and NMFS 1996). While much debate has centered on identifying units below the species level, it has become increasingly clear that examination of multiple character systems (i.e., multiple lines of evidence) and the processes that influence their diversification is necessary to

accurately delineate units for conservation. For example, many studies based on single lines of evidence, whether genetic sequence data or morphology, have been shown to be problematic once additional character sets have been examined (Janzen et al. 2002; Shaw 2002; Babik et al. 2005). Although no universally accepted criteria exist for recognizing subspecies, units such as evolutionary significant units (ESU) have been widely used for delineating conservation units (Moritz 1994; Crandall et al. 2000; Haig et al. 2006). In principle, an ESU is one or more population units with a distinct long-term evolutionary history (potentially exhibiting adaptive divergence) that is separate from other population units (Ryder 1986). Thus, ESUs are the primary source of historical genetic diversity within a species that merit special consideration in conservation efforts. However, operational genetic criteria for recognizing ESUs have differed. Moritz (1994) defined ESUs as groups of populations that are "reciprocally monophyletic for mtDNA alleles and show significant divergence of allele frequencies at nuclear loci". In contrast, Crandall et al. (2000) used a heuristic study of 8 separate cases to establish criteria and management recommendations for ESU designation on the basis of genetic, ecological, recent, and historical information.

We examined mitochondrial DNA (mtDNA) genetic variation to test hypotheses concerning the evolutionary history of *Chionactis occipitalis* (Western Shovel-nosed Snake) and gain insight into processes driving the distribution of genetic diversity within this species. We specifically focused on whether currently recognized subspecies constitute naturally defined ESUs. For example, valid subspecies should exhibit exclusive or near-exclusive patterns based on mtDNA markers and other lines of evidence (such as morphological or ecological divergence). Discordance between mtDNA and current subspecies designations would suggest that further data are needed to clarify the biological validity of these taxonomic distinctions.

Chionactis occipitalis is a small colubrid snake inhabiting arid valley floors and bajadas of the Mojave, Colorado, and Sonoran deserts. Morphological assessments of taxonomy currently recognize four subspecies: *C. o. occipitalis* (Mojave Shovel-nosed Snake), *C. o. annulata* (Colorado Shovel-nosed Snake), *C. o. talpina* (Nevada Shovel-nosed Snake), and *C. o. klauberi* (Tucson Shovel-nosed Snake). The subspecies are distinguished partly by ventral scale counts and number of dark bands encircling the body, but the most striking variation is in pattern and coloration of secondary bands (Stickel 1941; Klauber 1951). *Chionactis o. klauberi* has the most restricted range of the subspecies (Klauber 1951), known historically from desert valleys of the Sonoran Desert in south-central Arizona (Fig. 1). Population sizes and range for this putative subspecies have declined significantly over the past 25 years due to substantial habitat loss (through agriculture and urbanization), and existing populations are further threatened by expansion of the Tucson and Phoenix metropolitan areas (Rosen 2003). These factors prompted a petition (Center for Biological Diversity 2004) to list the subspecies as endangered under the U. S. Endangered Species Act. However, the validity of *C. o. klauberi* is complicated by a purported zone of intergradation with *C. o. annulata* across central Arizona (Klauber 1951). Further, the criteria used by Klauber and others to designate subspecies of *C. occipitalis* are largely considered inadequate today. These include the treatment of subspecies as geographical variants with weak morphological differentiation, often assumed *a priori* to intergrade into one another. For example, Klauber considered the composite character "number of dark bands on the body plus unmarked anterior band positions on the ventrum" to be the most important numerical character distinguishing *C. o. annulata* from *C. o. occipitalis* and arbitrarily assigned a threshold that defined *C. o. annulata* as having "usually fewer than 45". He further observed that about 20% of *C. o. occipitalis* specimens fell below this criterion and about 10% of *C. o. annulata* specimens have 45 or more. Thus, such designations were apparently established primarily for the purpose of elucidating gradients of variation as opposed to delineating discrete taxa.

Chionactis occipitalis annulata occurs within the Lower Colorado Subdivison of the Sonoran Desert in southeastern California and extends eastward where it forms a broad zone of contact with *C. o. klauberi* across Maricopa and southwestern Pima Counties, Arizona (Fig. 1; Klauber 1951). These two subspecies differ in morphology: both have black primary dorsal bands and red secondary bands, but *C. o. klauberi* also possesses black maculations between the primary band interspaces. However, specimens taken from within the purported intergrade zone are often difficult to unambiguously assign to a taxon, since subspecies delimitation in *Chionactis* was generally based on trends in morphological variation as opposed to diagnosis (Stickel 1941; Klauber 1951; see also Douglas et al 2002). Without any analytical basis, Stickel (1941) referred to a specimen collected near Wickenburg, AZ as *C. o. annulata* whereas Klauber (1951) considered this same specimen a *C. o. annulata*-*C. o. klauberi* intergrade. The processes underlying this geographic variation are of interest for both evolutionary and conservation biology. If *C. o. klauberi* possess *C. o. annulata* mitochondrial haplotypes as the result of either introgression or recent shared history (i.e. haplotypes from each subspecies are not exclusive with respect to each other), then all collection sites of *C. o. klauberi* including locations within the putative intergrade zone may be nested within a larger ESU, applying the criteria of Moritz (1994). However, if

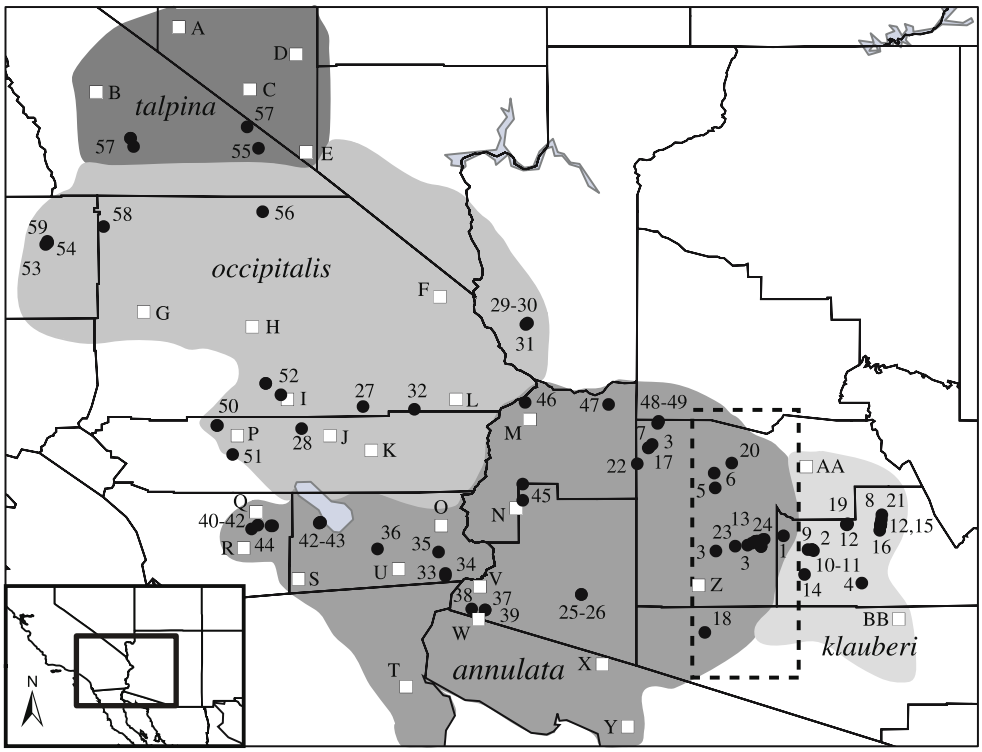

Fig. 1 Generalized morphological subspecies ranges of *Chionactis occipitalis*. Shaded areas represent each subspecies range based on Stickel (1941) and Klauber (1951). Black points correspond to molecular collection locations examined and numbers correspond to mtDNA haplotypes observed at each collection location. White squares correspond to the morphologically defined populations designated by Cross (1979) and used in our morphology analyses. The letter next to each square corresponds to Table 1. The dashed box outlines the approximate morphological intergrade zone observed between *C. o. annulata* and *C. o. klauberi*

haplotypes from collection locations on opposite sides of the intergrade zone form monophyletic genetic lineages then designation of *C. o. klauberi* populations as a separate unit may be considered valid.

Our main goal was to explore evolutionary relationships and boundaries among subspecies of *C. occipitalis*, with particular focus on individuals within the known range of *C. o. klauberi*. We used mitochondrial DNA sequences from specimens collected throughout the entire range to construct a molecular phylogenetic hypothesis for *C. occipitalis*. We also reanalyzed 14 morphological characters taken from an unpublished morphological assessment of *C. occipitalis* (Cross 1979). On the basis of these two data sets, we addressed the following: 1) Do the current subspecies designations represent distinct lineages? 2) Where do possible barriers to gene flow exist? 3) Are populations of *C. occipitalis* found in south-central Arizona (currently designated as *C. o. klauberi*) differentiated from populations throughout the rest of the species range?

Materials and methods

Molecular phylogenetic analysis

For the molecular analysis, we obtained tissue samples of 81 specimens of *Chionactis occipitalis* from 73 collection localities throughout California and Arizona (Fig. 1; Appendix 1). Sampled localities generally represent the distributional range of the species and include all formally recognized subspecies. We were unable to obtain samples from Nevada or Mexico.

Genomic DNA was extracted from ethanol-preserved tissues (liver, muscle, and tail tips) using standard DNA extraction techniques (Hillis et al. 1996) or Qiagen DNeasy extraction kits (Qiagen Inc., Valencia, CA, USA). Portions of the mitochondrial ND1 protein coding gene and the 16S rRNA coding gene were amplified using polymerase chain reaction (PCR) and the following primers: 16dR (5′-CTACGTGATCTGAGTTCAGACCGGAG-3′) and tIle-R (5′-TCTCRGGCACAYTTCCATTGTGGT-3′). Approximately 50–100 ng of total DNA was used as template for PCR in a final volume of 25 µl containing 1.5 mM $MgCl_2$, 0.2 mM dNTPs, 0.2 µM of each primer, 1X PCR buffer (invitrogen), and 1 unit of Platinum® *Taq* DNA Polymerase. Thermal cycling conditions consisted of an initial denaturing and enzyme activation step at 94°C for 2 min followed by 35 cycles of denaturing at 94°C for 30 s, annealing at 51°C for 30 s, and extension at 72°C for 1 min. PCR products were purified and directly sequenced on an ABI 3100 capillary system. Sequences were edited using Sequencher™ 4.5 and aligned using Clustal X (Thompson et al. 1997). To aid in the identification of possibly ambiguously aligned insertions/deletions positions within the 16S segment, the sequences were aligned using various opening gap costs (=6, 9, 12) implemented by Clustal X.

Nucleotide positions that were aligned differently under any of the gap opening costs were considered ambiguous and were excluded from analyses (Gatesy et al. 1993).

Phylogenetic relationships among mtDNA haplotypes were estimated using Bayesian inference and maximum parsimony (MP). Bayesian phylogenetic analyses were implemented using the program MRBAYES 3.1.2 (Huelsenbeck and Ronquist 2001). Given the potential heterogeneity of DNA sequence evolution within and/or across genes, the mtDNA data were divided into four data partitions: three for each codon of the protein coding ND1 and one for the 16S region (Nylander et al 2004; Brandley et al. 2005). Only a single partition (vs. separate stem and non-stem partitions) was used for the 16S data because it consisted of only 160 bp and ~85% of those represent non-stem forming positions. An appropriate model of sequence evolution for each partition was determined using Akaike information criterion (AIC) implemented with MrModeltest version 2.2 (Nylander 2002). Two simultaneous, independent analyses were run to help determine when convergence had been achieved (i.e. when average likelihood scores, $-\ln L$, from the two runs differed by less than a few tenths of a point). Each analysis consisted of 1.0×10^7 generations with the first 500,000 generations discarded as burn-in (i.e. the number of generations at which convergence was achieved). Clades with posterior probabilities (*Pp*) of ≥0.95 were considered strongly supported (Alfaro et al. 2003). MP analyses were implemented in PAUP* 4.0b10 (Swofford 2002) using an unweighted heuristic search option with 5,000 pseudo-replicates (10 random addition of sequences per pseudo-replicate), tree-bisection-reconnection branch swapping, and gaps coded as missing data. Confidence of inferred clades from MP was assessed using nonparametric bootstrapping (Felsenstein 1985). Nodes with bootstrap values of ≥70% were considered strongly supported (Hillis and Bull 1993). Following the outgroup method, *Chionactis palarostris*, the closest relative of *C. occipitalis* (Klauber 1951; Mahrdt et al. 2001), was used to infer the root of the phylogram for both Bayesian and MP analyses.

Nested clade phylogeographical analysis (NCPA) was used on a subset of our data to test for significant associations between genetic variation and geography, and to distinguish among alternative potential causes of such geographical associations (Templeton 2004). To implement NCPA, we used the Templeton et al. (1992) haplotype network estimation, as implemented in the TCS v1.21 software of Clement et al. (2000), to resolve intraspecific relationships for haplotypes recovered. This method estimates the maximum number of mutational steps among haplotypes as a result of single substitutions with a 95% statistical confidence (described in Templeton et al. 1992). The recovered network was input into GEODIS v2.5 (Posada et al. 2000) together with geographic sampling information, and the NCPA method was then used to infer the underlying population processes for each clade that demonstrated a significant geographical association. If a significant departure from simulated randomness was observed in the distance measures, then the null hypothesis (i.e. panmixia) could be rejected. The statistical results were then used to make population structure inferences following the most recent inference key of Templeton (2004).

Landscape genetic analyses

To test for spatially limited genetic connectivity (i.e. isolation by distance) among collection localities we estimated the correlation between mtDNA sequence divergence and geographical distance between collection localities with Isolation By Distance, Web Service (Jensen et al. 2005) using a nonparametric Mantel test and statistical significance assessed with 10,000 randomizations. Estimates of average pairwise sequence divergence between all collection locality pairs, corrected using the Kimura (1980) 2 parameter model of evolution, were calculated using ARLEQUIN v3.0 (Excoffier et al. 2005) and assessed against the straight-line geographical distance.

We created an interpolated genetic landscape surface to examine the existence and approximate location of barriers to gene flow. Using the program Alleles In Space (Miller 2005), we generated a connectivity network among sample locations based on pairwise geographic distances using the Delaunay triangulation method (i.e. each collection point was connected in a straight line to its nearest neighbors, creating a triangular network with no overlapping lines). The genetic distances between pairs of collection locations were then plotted at the geographic midpoints between collection locations along the network. Next, we took this output from Alleles In Space and performed an inverse distance weighted interpolation of genetic distances in ArcGIS 9.1 to obtain a graphical representation of genetic distance patterns that could be overlaid onto our sampling map. This resulted in a genetic landscape that was visualized within a color gradient from red to blue, where red represents highest genetic differentiation and blue represents lowest genetic differentiation. We interpolated over residual genetic distances to ensure that areas of high genetic differentiation were not merely interpolated due to the fact that one or a few collection areas were geographically isolated (Miller et al. 2006).

Finally, we examined whether certain environmental factors may explain genetic differentiation among collection locations using a distance-based redundancy analysis (dbRDA; Legendre and Anderson 1999; McArdle and Anderson 2001). This is a multivariate multiple regression performed directly on a dissimilarity or distance response

matrix, such as pairwise genetic distances, in two steps (e.g. Geffen et al. 2004; Pilot et al. 2006). First principal coordinate analysis is performed on the distance matrix, followed by redundancy analysis of a matrix of independent variables and the multivariate response matrix (consisting of the principal coordinates). In dbRDA, collection sites, rather than individual distances, are treated as the units for analysis.

As with IbD analyses described above, we calculated genetic distance as the average pairwise sequence divergence among collection locations and performed dbRDA on three sets of collection locations: all collection locations (73 localities), and separately within the southeastern (59 localities) and the northwestern (14 localities) clades revealed from our Bayesian analysis. We tested for dependence of genetic distances on several sets of environmental predictors. These were 1) geographic location (latitude and longitude); 2) desert basin (Mojave, Sonoran, and Colorado, Bailey et al. 1994); 3) land cover type (shrub/scrub, grassland, pasture, cropland or barren, 2001 National Landcover Database); 4) temperature (average minimum January temperature and average maximum July temperature, 1950–2004 PRISM, Spatial Climate Analysis Center, Oregon); 5) average annual rainfall (1961–1990 PRISM; USDA NRCS National Water and Climate Center); and 6) elevation (Seamless Shuttle Radar Topography Mission 3 Arc Second, NASA). These environmental variables were extracted from a GIS for all collection location points. Source environmental data layers are publicly available from the EROS Seamless Data Distribution Center (http://seamless.usgs.gov/) and from the National Atlas (www.nationalatlas.gov).

In the program DISTLM v. 5 (Anderson 2004), we performed marginal tests on individual sets of predictor variables to identify those variables that were correlated with genetic distance. Significance was assessed with 10,000 unrestricted, simultaneous permutations of the rows and columns of the distance matrix. Second, we performed conditional tests for each set of predictors, with latitude and longitude included as covariables in the model. This allowed us to determine the extent to which any set of predictor variables explains genetic divergence beyond that explained by geographic distance alone. Significance for conditional tests was assessed using 10,000 permutations of the rows and columns of the distance matrix under the reduced model.

Morphology

The most recent published morphological assessments of *Chionactis* were those of Stickel (1941) and Klauber (1951). Stickel (1941) described *C. o. klauberi* and treated *C. palarostris* as a subspecies of *C. occipitalis*. Klauber (1951), who originally described *C. palarostris* in (1937), once again recognized the taxon as a distinct species and described *C. o. talpina* based on new material from the northern Mojave Desert. To date, the most comprehensive study of geographic variation in the morphology of *Chionactis* was undertaken as a doctoral dissertation by Cross (1979), but this work has remained unpublished. We augmented our study of genetic variation in *C. occipitalis* by compiling and re-analyzing these unpublished morphological data. Because Cross (1979) did not provide raw data for the 1543 specimens he examined, we were restricted to data summaries for 32 populations that he designated through consideration of specimen provenance and geography. These include 28 populations from throughout the distribution of *C. occipitalis* and 4 populations assigned to the more narrowly distributed *C. palarostris* (Fig. 1; Table 1). Taxonomic assignment of populations follows Klauber (1951). Population Z was considered *C. o. klauberi* by Cross (1979) but falls within the purported intergrade zone between *C. o. klauberi* and *C. o. annulata* as circumscribed by Klauber (1951).

Although there is not strict overlap between collection localities from both the morphological and genetic datasets, there is sufficient spatial concordance to make general comparisons between morphological and genetic patterns. We included data on *C. palarostris* to increase statistical sampling as well as for comparative purposes, since *C. palarostris* has long been recognized as the sister species to *C. occipitalis*. Cross (1979) reported a large sex bias in *Chionactis* specimens in collections with two to three times as many males as females. He also demonstrated that geographical patterns in morphology were congruent for males and females, albeit somewhat weaker for females. For these reasons, and to avoid confounding influence of sexual dimorphism, we opted to limit our analyses to male means for each of the designated populations.

The dataset included 14 quantitative variables that were amenable to reanalysis from the Cross (1979) dissertation (Appendix 2). Taxonomic characters related to color and interspace maculations were not available, since these characters fade rapidly in preservative. We utilized a multivariate approach to data analysis under the assumption that geographic covariation of multiple characters is more likely to reflect the consequences of population-diversifying mechanisms than patterns of variation in single characters (Wüster et al. 2001; Coyne and Orr 2004; Osada and Wu 2005).

We used non-metric multidimensional scaling (NMS) to explore broad patterns of morphological variation among *C. occipitalis* and *C. palarostris*. NMS is a robust, iterative ordination technique that preserves rank ordering of distances; thus any distance measure can be used in its

Table 1 Populations of *Chionactis occipitalis* and *C. palarostris* designated by Cross (1979) and herein used for assessment of morphological variation. Subspecies taxonomy follows Klauber (1951) and clade affiliation was based on the geographic boundaries of the two major clades revealed in our Bayesian analysis

Population	Locality	Taxon	Clade
A	Sarcobatus Flats, Nye Co., NV	*C. o. talpina*	Northwestern
B	Saline Valley, Inyo Co., CA	*C. o. talpina*	Northwestern
C	Amargosa Desert, Nye, Co., NV	*C. o. talpina*	Northwestern
D	Nevada Test Site, Nye Co., NV	*C. o. talpina*	Northwestern
E	Pahrump Valley, Clark/Nye Co. NV	*C. o. talpina*	Northwestern
F	Piute Valley, Clark Co. NV and San Bernardino (SB) Co., CA	C. o. occipitalis	Incertae sedis
G	Mojave River, SB Co., CA	C. o. occipitalis	Northwestern
H	Pisgah Crater, SB Co., CA	*C. o. occipitalis*	Northwestern
I	Twentynine Palms, SB Co., CA	*C. o. occipitals*	Northwestern
J	Pinto Basin, Riverside Co., CA	*C. o. occipitalis*	Southeastern
K	Desert Center, Riverside Co., CA	*C. o. occipitalis*	Southeastern
L	Vidal Valley, SB Co., CA	*C. o. occipitalis*	Southeastern
M	Parker-Bouse, La Paz Co., AZ	*C. o. annulata*	Southeastern
N	Palm Canyon, La Paz Co., AZ	*C. o. annulata*	Southeastern
O	Midway Well, Imperial Co., CA	*C. o. occipitalis*	Southeastern
P	Coachella Valley, Riverside Co., CA	*C. o. occipitalis*	Northwestern
Q	Borrego Valley, San Diego (SD) Co., CA	*C. o. annulata*	Southeastern
R	La Puerta Valley, SD Co., CA	*C. o. annulata*	Southeastern
S	West Mesa, Imperial Co., CA	*C. o. annulata*	Southeastern
T	San Felipe, Baja California, MX	*C. o. annulata*	Southeastern
U	Algodones Dunes, Imperial Co., CA	*C. o. annulata*	Southeastern
V	Yuma Mesa, Yuma Co., AZ	*C. o. annulata*	Southeastern
W	Gran Desierto, Sonora, MX	*C. o. annulata*	Southeastern
X	Los Vidrios Dunes, Sonora, MX	*C. o. annulata*	Southeastern
Y	Shell Dunes, Sonora, MX	*C. o. annulata*	Southeastern
Z	Ajo-Gila Bend, Pima and Maricopa Co., AZ	*C. o. annulata-klauberi*	Southeastern
AA	Avra Valley, Pima Co., AZ	*C. o. klauberi*	Southeastern
BB	Phoenix, Maricopa Co., AZ	*C. o. klauberi*	Southeastern
–	Organ Pipe Cactus NM, Pima Co., AZ	*C. palarostris*	Pala.
–	Altar, Sonora, MX	*C. palarostris*	Pala.
–	Central coastal Sonora, Sonora, MX	*C. palarostris*	Pala.
–	Sonoran Plains, Guaymas, Sonora, MX	*C. palarostris*	Pala.

computation. Furthermore, since NMS is an iterative method (as opposed to Eigen analysis), assumptions of data normality and linearity are relaxed. We ran a preliminary analysis to determine dimensionality of the data and initial position of populations in multivariate space. We then performed the NMS analysis starting with these configurations, selecting two dimensions and 400 iterations for our final solution. We visualized morphospace occupation by plotting population scores for each axis, considering both traditional taxonomy (Klauber 1951) and the most divergent clades defined by our mtDNA data. We performed NMS with PC-ORD 4 (McCune and Mefford 1999) using Sorenson distances.

Results

Molecular phylogeny

We obtained sequences for 81 *Chionactis occipitalis* and one sequence from *C. palarostris* for outgroup purposes. A total of 1098 base pairs of mtDNA (165 bp 16S rRNA and 933 bp ND1) were unambiguously aligned and used for subsequent analyses. Among these sites, 205 were variable among *Chionactis* sequences and 157 were parsimony informative. For the *C. occipitalis* examined, 59 unique haplotypes were identified (Appendix 1). Uncorrected sequence divergence among *C. occipitalis* haplotypes

ranged from 0.09% to 6.68% (mean 3.78%; Table 2). Sequence divergence estimates between *C. occipitalis* and its nearest relative (*C. palarostris*) range from 5.62–8.22% (mean 6.72%).

The model of sequence evolution selected using AIC varied by data partition: 16S = GTR + I; ND1–first codon position = GTR + I; ND1-second codon position = HKY + I; ND1-third codon position = HKY + G. The two independent partitioned analyses converged on similar average log-likelihood values (-ln L = 3573.01 and 3573.43). A 50% majority rule consensus tree of Bayesian analyses is shown in Fig. 2. MP analyses resulted in concordant topologies and corresponding posterior probabilities (Pp) and MP bootstrap values for clade relationships are shown in Fig. 2. The most obvious feature of our tree is the division of haplotypes into two major lineages (northwestern and southeastern) and six minor subclades (A-F). The northwestern clade includes collection localities primarily in the western Mojave Desert of California within Riverside, San Bernardino, Kern, and Inyo Counties but also includes collection sites from the northern Coachella Valley. The southeastern clade includes more widely distributed collection localities across the Sonoran Desert of California and Arizona, as well as a portion of the eastern Mojave Desert. The two clades approach one another in the Coachella Valley region of California. However, given our limited sampling within this region we were unable to determine the location(s) and geographic extent of contact.

The two clades differ in degree of resolution and nodal support (Fig. 2). Within the northwestern clade, two subclades were identified (A and B). Subclade A (haplotypes 50–51) occupies a small area restricted to the northern portion of the Coachella Valley in Riverside County, California. The range of subclade B (haps 52–59) is more geographically widespread extending from the eastern portion of the Transverse Ranges, northward across the Mojave Desert. However, the relationship between the two subclades is not strongly supported ($Pp < 0.5$). Bayesian trees within the 95% credible set reveal subclade A to be either nested within the northwestern clade (shown in Fig. 2), or paraphyletic with respect to all other *C. occipitalis* haplotypes. In contrast, the southeastern clade is well supported, but the relationships between the subclades exhibit varying levels of support. Subclade C and D (haps 33–49) contain haplotypes extending along the Colorado River Valley of California and southern Arizona, and a geographically disjunct group to the north in western Arizona (Yuma, La Paz, and Maricopa Counties). Subclade E and F (haps 1–32) form two geographically discontinuous units: subclade E (haplotypes 27–32) extends along a northeastern axis from Riverside County, California into Mohave County, Arizona, and subclade F (haplotypes 1–26) forms a group of recently diverged haplotypes, as evidenced by the shorter branch lengths, that extend across Arizona (Pima, Pinal, Maricopa, and Yuma Counties).

Table 2 Pairwise comparisons of average uncorrected sequence divergence within (along diagonal) and among (below diagonal) the Northwestern and Southeastern clades

Clade	Northwestern	Southeastern
Northwestern	3.2%	–
Southeastern	5.4%	3.1%

We restricted NCPA to a subset of the data (subclade F) for which we had relatively dense geographical sampling, corresponding to thirty-six collections sites of *C. o. annulata* and *C. o. klauberi* and the purported zone of intergradation between them. Haplotypes were connected by TCS using a 95% parsimony limit that imposed a maximum of 14 mutational steps between connections (Fig. 3a). Of the eight "nesting clades" that included both geographical and genetic variation (clades 1–1, 1–2, 1–4, 1–6, 2–1, 2–2, 3–1, 4–1), we could reject the null hypothesis of no statistical association between haplotype distributions and geography in five cases (clades 1–6, 2–1, 2–2, 3–1, and 4–1; Table 3). In general, most clade distances (D_C) were significantly small, indicating that the geographic spread of haplotypes within a given clade were restricted. Range expansion was also inferred for clade 3–1 as a potential driving force in haplotype distributions across central Arizona (Fig. 3b; Table 3). No definitive conclusions (i.e. restricted gene flow or contiguous range expansion) could be drawn at the highest clade level (clade 4–1) because of the ambiguity in determining interior/tip status.

Landscape genetic analyses

Mantel tests for IbD were performed on all collection localities, within the two major clades, and on clades 4–1 and 3–1 from the NCPA. Results from our IbD analyses produced similar results as our NCPA analyses. IbD analyses revealed a significant positive relationship between genetic differentiation and geographic distance for: all collection localities ($r = 0.626$, $P \leq 0.001$), Northwestern Clade ($r = 0.429$, $P \leq 0.002$), Southeastern Clade ($r = 0.693$, $P \leq 0.0001$), and clade 4–1 ($r = 0.386$, $P \leq 0.005$). However, the significant relationship within clade 4–1 appeared to be driven by the large sampling gap between the Mohawk Dune collection site (haplotypes 25–26) and all other sites to the east that include both *C. o. annulata* and *C. o. klauberi* localities. When Mohawk Dune samples were excluded, the results were non-significant ($r = 0.077, P \leq 0.281$) consistent with

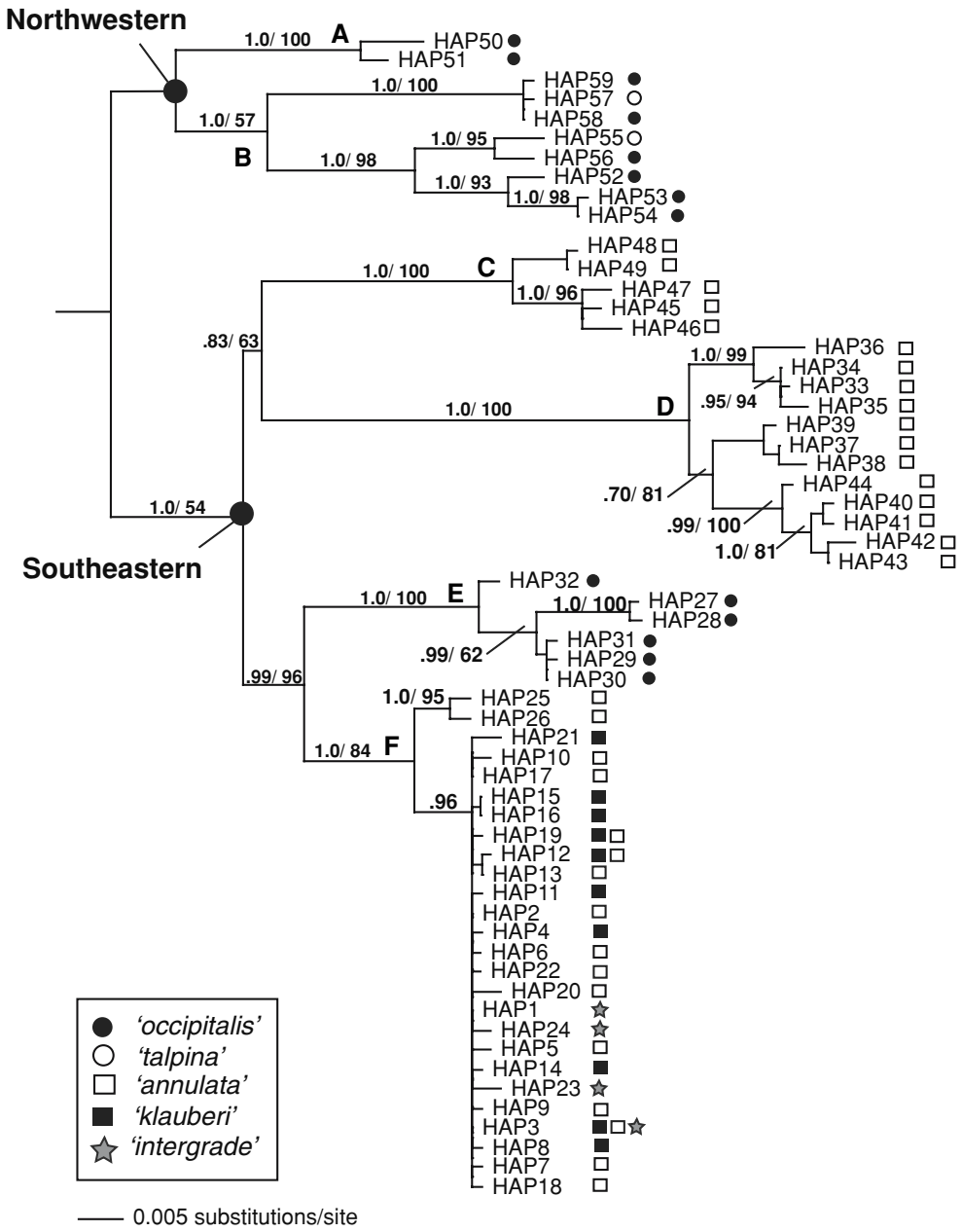

Fig. 2 Phylogram from the Bayesian analysis of the mtDNA sequence data. List of haplotypes, subspecies affinities, and their geographic locations are found in Appendix 1. The numbers on branches indicate Bayesian posterior probabilities (*Pp*) and MP bootstrap percentage values (respectively). Clades with $Pp \geq 0.95$ and MP bootstrap values ≥70% were considered strongly supported

our NCPA and suggesting recent expansion and/or drift across collection sites of central-eastern Arizona (clade 3–1; Fig. 3b).

The interpolated genetic landscape revealed highest genetic distances (after accounting for geographical distance) associated between collection locations separated by mountains and/or across abrupt shifts in elevation (e.g. opposite sides of the Transverse Mountain Range, separating the comparatively low elevation Colorado Desert to the south from the higher Mojave Desert to the north), while lower genetic distances were revealed between collection localities found within the same basin and/or areas with less topographic complexity between them (Fig. 4).

Finally, the results of the distance-based redundancy analysis suggest strong correlations between all of the sets of environmental variables and the genetic distance matrix both in the total dataset and in the southeastern clade, and for all variables except elevation in the northwestern clade (Table 4). In all three analyses, desert basin explained the largest amount of variation in genetic distance (51% in the total dataset, 72% in the southeastern clade and 44% in the

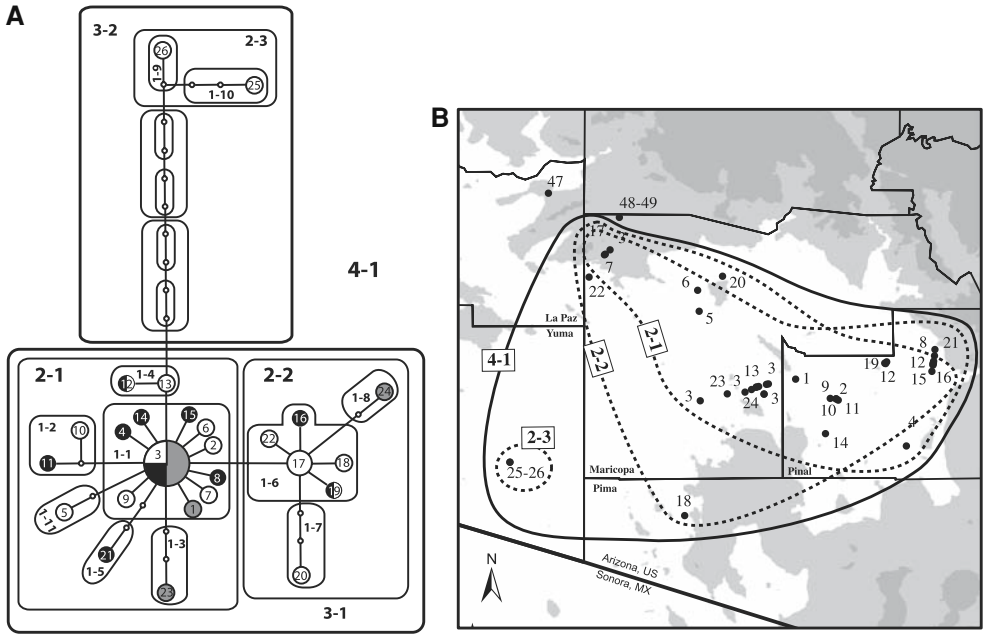

Fig. 3 Nested clade phylogeographical analysis of subclade F. (**a**) The inferred relationships of haplotypes and nesting groups using TCS. Haplotype numbers are the same as those in Figure 2. Relative proportion of haplotypes from snakes identified as *C. o. annulata*, *C. o. klauberi*, and intermediates are colored white, black, and grey respectively. Each line represents a single mutational step connecting two haplotypes. Small open circles indicate haplotypes states that are necessary intermediates but were not present in the sample. (**b**) Geographic distribution of haplotypes and nesting clades across Arizona. Shading indicates elevation with light grey between 600 and 1,000 m, dark grey above 1,100 m

northwestern clade). In the conditional tests, desert basin, temperature, and elevation remained strongly associated with genetic distance in the total dataset (explaining 13%, 5%, and 6% of the remaining variation in genetic distance, respectively). In the southeastern clade, significantly associated variables were limited to desert basin and elevation (explaining 24% and 3% of the variation, respectively; Table 4), and in the northwestern clade, only desert basin explained a significant proportion of the remaining variation (30%) after accounting for geographical distance (Table 4). Although none of these variables were highly correlated with each other ($r < 0.90$), some general associations between desert basins and climatic variables exist. Desert basins are defined by a combination of temperature, precipitation, vegetation, and terrain features (Bailey et al. 1994), and the Mojave basin is generally higher in elevation than the Sonoran and Colorado. When desert basins were overlaid on our interpolated genetic landscape, these boundaries were broadly concordant with the areas of highest genetic divergence seen in our interpolated genetic landscape (Fig. 4).

Morphology

The NMS ordination had a final stress of 5.96 and final instability of 0.00001. Stability of the solution was reached after only 70 iterations and the final ordination accounted for 96.7% of the variation in the dataset (Axis 1 = 81.5%; Axis 2 = 15.2%). Variable scores for both axes are presented in Table 5. In contrast to the unambiguous separation between populations of *C. palarostris* and *C. occipitalis*, the ordination revealed only weak differentiation of populations within *C. occipitalis* (Fig. 5). At the broadest scale (mtDNA clades), morphological variation in the southeastern clade largely overlapped and greatly exceeded that of the northwestern clade. Among traditional subspecies, similar patterns were recovered. Populations of *C. o. annulata* and *C. o. talpina* exhibited the greatest and most diffuse variation, while populations of *C. o. occipitalis* and *C. o. klauberi* were relatively cohesive. The variation in *C. o. talpina* completely encompassed variation observed in *C. o. occipitalis*. Four populations of *C. o. annulata* encroached into ordination space occupied by *C. o. occipitalis/talpina*: two populations from east of the Pinacate massif (Populations X and Y), and two populations from west-central Arizona (Populations M and N). The populations from west-central Arizona are geographically contiguous with populations of *C. o. occipitalis* in California, whereas the Pinacate populations are at the southern periphery of the distribution of *C. o. annulata* in northern Sonora, Mexico. Population P (Coachella Valley) was placed well within the cluster of *C. o. occipitalis* populations and distant to other populations from the Colorado Desert (traditionally assigned to *C. o. annulata*).

Table 3 Results of the nested clade phylogeographical analysis for subclade F. Nesting clades and clades are shown in Fig. 3

Nesting clade	Clades	DC[a]	DN[a]	Inference[b]
1–6	Hap16	0	88	
	Hap17 (I)	0	105	
	Hap18	0	108	
	Hap19	0.6^{S}	64^{S}	
	Hap22	0	104	
	I-T	-0.3^{S}	22	1–2–3–4-No Restricted Gene Flow w/IbD
2–1	1–1 (I)	55	56	
	1–2	0^{S}	24^{S}	
	1–3	0	47	
	1–4	26	47	
	1–5	0.2^{S}	64	
	1–11	0	69	
	I-T	46^{S}	8	1–2–3–4-No Restricted Gene Flow w/IbD
2–2	1–6 (I)	89^{L}	89^{L}	
	1–7	0	51	
	1–8	2.7	22^{S}	
	I-T	87^{S}	57^{S}	1–2–3–4-No Restricted Gene Flow w/IbD
3–1	2–1 (I)	54	55	
	2–2	73^{L}	73	
	I-T	-18^{S}	-18	1–2–11–12-No Contiguous Range Expansion
4–1	3–1 (I)	59^{S}	59^{S}	
	3–2	0^{S}	159^{L}	
	I-T	59	-99^{S}	1–2 Inconclusive Outcome Tip/Interior Status Unknown

[a] Statistical significance of D_C and D_N determined by 10,000 random permutations of clades against sampling location. Superscript S/L corresponds to significantly small distance/large distance at $P \leq 0.05$ level. Interior clades are labeled with "(I)"

[b] Inferences were made following the updated version (11-Nov-2005) of the inference key provided in Templeton (2004). "IbD' refers to Isolation by Distance

The NMS ordination revealed that *C. o. klauberi* occupied a unique region of morphospace and is differentiated from other populations along a combination of the first and second axes; however, *C. o. klauberi* was positioned at the periphery of morphospace occupied by *C. occipitalis* and these populations do not form a distinct group clearly separated from other populations (Fig. 5). Variation in *C. o. klauberi* along Axis 1 (which accounted for 81.5% of morphological variation) broadly overlapped that of *C. o. annulata* (5 out of the 11 populations designated as *C. o. annulata* overlapped in NMS scores with *C. o. klauberi*). Furthermore, the morphological differentiation was greater among various populations within *C. o. annulata* than it was between populations of *C. o. klauberi* and *C. o. annulata*.

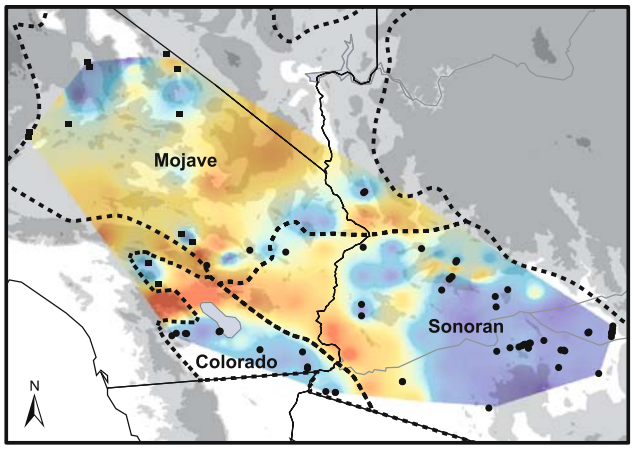

Fig. 4 Results of the genetic landscape interpolation analysis revealing genetic differentiation between pairs of collection locations. Genetic differentiation is plotted at the geographic midpoint between sample locations: red indicates highest genetic differentiation, blue represents lowest genetic differentiation. The dots and squares represent collection localities found in the Southeastern clade and Northwestern clade, respectively. Shading underneath indicates elevation with light grey between 600 and 1,000 m and darker grey between 1,100 and 2,000 m, and darkest grey above 2,000 m. The geographic boundaries of desert basins, as defined by Bailey et al. (1994), are indicated by the dotted lines

Discussion

The phylogenetic analysis of individuals across the distributional range of *Chionactis occipitalis* permitted us to resolve patterns of genetic structure and diversity that suggested the influence of historical climate change, probable isolation, and periods of habitat connectivity. Of particular importance was the detection of two primary clades within the species' range. Our Bayesian phylogram indicated generalized support for the presence of a group of west Mojave haplotypes that were distinct from those detected among Sonoran/Colorado and eastern Mojave Desert locations, and these lineages harbor high levels of sequence divergence between them (Table 2). Taken at face value, the general genealogical pattern is indicative of fragmentation. However, given that geographical sampling was scarce in the geographic region of contact between these lineages we were unable to discriminate fragmentation from isolation by distance. We discuss these patterns and their historical basis in more detail below. Lastly, our

Table 4 Tests for relationships between the genetic structure of Shovel-nosed snakes at different collection locations and sets of predictor variables, using the dbRDA multivariate F-statistic. Marginal tests are shown on the left. Conditional tests (including the latitude and longitude as covariables) are shown in the right columns. *P* indicates the probability values. %Var indicates the percentage of the multivariate genetic variation explained by the particular set of predictor variables. Results are reported for all data combined, within the Southeastern clade, and within the Northwestern clade

Variable set	Marginal tests			Conditional tests		
	F	p	% Var	F	p	% Var
All Data (73 locations)						
Desert Basin	36.6648	0.0001	51.16	11.4251	0.0001	13.36
Location	30.8765	0.0001	46.87	–	–	–
Elevation	16.2272	0.0001	18.60	9.3054	0.0001	6.31
Temperature	7.1806	0.0001	17.02	3.8352	0.0003	5.39
Cover Type	2.3869	0.0052	12.31	1.0709	0.387	3.24
Average Rainfall	7.9593	0.0002	10.08	1.4137	0.2041	1.07
Southeastern Clade (59 locations)						
Desert basin	70.3697	0.0001	71.54	32.8404	0.0001	23.57
Location	37.1992	0.0001	57.05	–	–	–
Elevation	25.9153	0.0001	31.26	4.4824	0.0095	3.24
Temperature	6.075	0.0005	17.83	1.6205	0.1504	2.43
Cover type	3.4507	0.0037	20.36	0.6785	0.6614	2.13
Average rainfall	11.9296	0.0001	17.31	2.1229	0.0911	1.60
Northwestern Clade (14 locations)						
Desert basin	9.4258	0.0031	43.99	8.2709	0.012	29.59
Location	2.9146	0.0269	34.64	–	–	–
Elevation	0.4654	0.6942	3.73	0.5621	0.5833	3.48
Temperature	3.7025	0.0062	40.23	2.0613	0.1722	20.53
Cover type	2.8118	0.0119	33.83	1.7520	0.1939	18.32
Average rainfall	2.5829	0.059	17.71	2.0020	0.1406	10.90

Table 5 Variable scores for the nonmetric multidimensional scaling (NMS) ordination. See Appendix 2 for variable definitions

Variable	Axis 1	Axis 2
LOR	−0.004	−0.024
VENT	0.022	0.015
CS	0.011	0.031
PTFB	−0.148	0.023
TB	0.179	0.025
HEM	−0.010	0.045
BB	0.161	0.010
UBPB	0.216	-0.062
DL	0.144	-0.046
OWHL	−0.028	−0.008
HLSVL	−0.021	−0.014
TAILTO	−0.005	0.012
FRONFL	−0.023	−0.004
FRONTN	0.026	0.008
% Variance	81.5	15.2

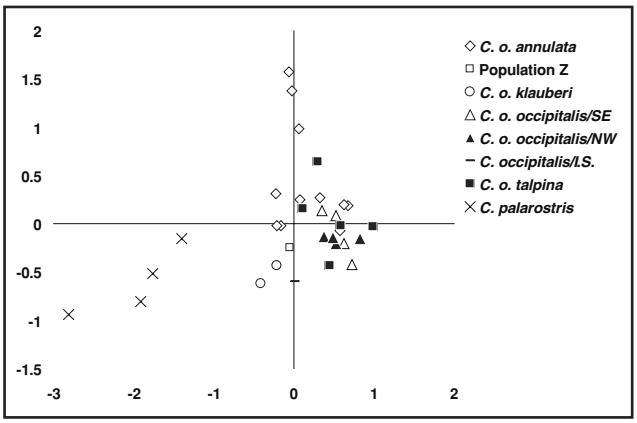

Fig. 5 Results of nonmetric multidimensional scaling (NMS) ordination based on 14 morphological variables. The analysis was based on population means (not individual specimens). Solid and open symbols represent populations within the Northwestern and Southeastern clades, respectively. Population Z lies in a putative intergrade zone between *C. o. annulata* and *C. o. klauberi* (see Fig. 1). C. o. occipitalis/I.S. refers to population F (Table 1), which we have considered *incertae sedis*

genetic and morphological analyses do not unequivocally support current subspecies designations. We compare/contrast these patterns and end with a discussion about the implications related to ESU status and conservation.

Phylogeography

The biogeographic history of arid adapted taxa in the desert southwest is complex, and evidence for multiple biotic refugia within this region is an increasingly common phenomenon (Van Devender et al. 1987; Douglas et al. 2006; Murphy et al. 2007). Overall, our analysis of *C. occipitalis* mitochondrial genetic variation appears to produce results superficially concordant to intraspecific variation observed in many other Mojave/Sonoran codistributed reptiles (i.e. *Crotalus*, Douglas et al. 2006; *Sceloporus magister*, Schulte et al. 2006; *Uma scoparia* and *Uma notata*, Trépanier and Murphy 2001; Murphy et al. 2007). In particular, mtDNA analyses of two species of rattlesnakes in the desert southwest (i.e. *Crotalus mitchellii* and *C. cerastes*; Douglas et al. 2006) demonstrated divergent lineages (comparable to levels in our study; >5%) at nearly the same location where strong mitochondrial genetic structuring occurs in *C. occipitalis* (Fig. 4). While the phylogenetic breaks between codistributed units in this region do not always align, the biogeographic fragmentation patterns across these species suggest they were influenced by similar isolating events. As support for geographically congruent phylogeographic structuring accumulates among diverse taxa in the desert

southwest, it will be possible to identify areas of evolutionary significance (sensu Avise 1996) that may be targeted for special conservation measures.

Although there are several possible explanations for the patterns of divergence seen in our data, we view two alternative hypotheses as the most relevant. The first hypothesis involves climatically induced Pleistocene effects. In effect, individuals from each clade persisted during periods of glaciation in distinct nonglaciated refugia in northern and southern regions of the southwestern warm desert system. Following glacial retreat, the separately diverged northwestern and southeastern lineages were able to re-expand and come into secondary contact to produce the genetic discontinuity observed. Although evidence for rapid climatic changes and distributional limits of the southwestern deserts during the Pleistocene comes primarily from vegetation histories derived from packrat middens, multiple studies have implicated Pleistocene glacial cycles as important diversification events in southwestern desert taxa (Ayoub et al. 2004; Douglas et al. 2006; Murphy et al. 2007). Thus, isolation between populations in the north and south may have been caused by the breadth and duration of the pluvial-interpluvial period (<2 mya) by repeatedly forcing snakes into isolated areas of nonglaciated refugia (sensu Ayoub et al. 2004). Two desert refugia have been postulated for arid adapted species in the southwest which correspond well with the lineage patterns of divergence for *C. occipitalis*: one in the Mojave Desert near Death Valley, and one in the Sonoran Desert near the lower Colorado River (Van Devender et al. 1987; Betancourt 2004).

Alternatively, the two lineages observed in *C. occipitalis* might not reflect geographical divergence due to an extrinsic historical barrier alone, but rather a combination of geographic, ecological and stochastic genetic causes. Recent simulations have demonstrated that low dispersal species can form distinct phylogeographical genetic groups due to the stochastic nature of the coalescent process, even when the species is continuously distributed (Irwin 2002). Isolation by distance was observed across collection sites and within lineages, suggesting limited dispersal abilities. In addition, our distance-based redundancy analysis indicated that isolation in different desert basins and/or differences in elevation and temperature among sites play major roles in the observed population structure. Under this hypothesis then, *C. occipitalis* may have been continuously distributed across the desert southwest and phylogeographical structure in mitochondrial DNA developed as a result of genetic drift and restricted gene flow between populations coupled with the development of each desert basin. Even after accounting for geographic distance, we found that desert basin was the strongest determinant of population differentiation both in the total dataset and within each major clade. This suggests that diversification across desert basins has occurred throughout the history of the species. While the observed genetic patterns could be consistent with the refugia hypothesis, it also indicates that ecological differences and elevation barriers among the basins are equally sufficient to maintain genetic differentiation, even among individuals within the same major clade. For example, high levels of genetic divergence within the southeastern clade were observed between subclade D and all other subclades (Fig. 2) and correspond to snakes inhabiting the Colorado versus the eastern Sonoran Desert Basins. In addition, the boundaries of the desert basins are spatially concordant with the areas of highest genetic divergence seen in our interpolated genetic landscape, further highlighting the importance of basin isolation (Fig. 4).

While reconstructing the evolutionary history of lineages in this region continues to be challenging, divergence patterns revealed in other co-distributed taxa may help to distinguish the relative importance of the alternative hypotheses suggested above. Although glaciation has been implicated as a likely determinant of historical population demographics for species inhabiting the desert southwest, our data suggest that both historical vicariance and more recent ecological and environmental isolating mechanisms may be at play, and consequently, future studies should consider both simultaneously.

Molecular and morphological patterns

Our phylogenetic analysis of the mtDNA data revealed significant geographical structuring of haplotypes and partitioned the haplotypes into two main clades, but with different geographical limits than established by traditional subspecies taxonomy. The northwestern clade consisted of snakes from the western Mojave Desert (including *C. o. talpina* and western populations of *C. o. occipitalis*), while the southeastern clade was composed of snakes from the Sonoran Desert (both *C. o. annulata* and *C. o. klauberi*) and eastern Mojave Desert populations of *C. o. occipitalis*.

Our morphological analysis using NMS did not provide strong evidence for differentiation of subspecies within *C. occipitalis.* Instead broad overlap was exhibited, with some geographic structure. With the exception of a single population from southern Nevada and adjacent California (Population F), phenotypic variation within *C. o. occipitalis* was entirely contained within variation in *C. o. talpina*. *Chionactis o. annulata* showed the greatest magnitude of variation, occupying areas of unique morphospace as well as showing some overlap with *C. o. occipitalis* and *C. o. talpina*. Populations assigned to *C. o. klauberi* formed a cohesive cluster, but were not

well separated from other populations of *C. occipitalis*. Thus on the basis of morphology, there is no justification for taxonomic recognition of *C. o. klauberi* as an entity separate from other *C. occipitalis* populations. However, the extinction of *C. o. klauberi* populations would result in a substantial reduction of total phenotypic variation within the species. Although our data are limited with respect to evaluating continuous versus abrupt geographic variation, the easternmost population of *C. o. klauberi* (Population BB from Avra Valley) is positioned at the endpoint of the ordination, whereas Population Z (considered an intergrade population by Klauber 1951) is situated closest to populations of *C. o. annulata* (Fig. 5). This pattern is consistent with a hypothesis of clinal variation.

Our molecular and morphological results fail to indicate concordant patterns with the traditional *C. occipitalis* subspecies taxonomy. There are at least two alternative explanations for this discordance (see Funk and Omland 2003). The first is that previous diagnoses and descriptions of subspecies reflect inadequate morphological taxonomy. Specifically, they do not represent the actual geographic distribution and evolutionary history of the major groups within *C. occipitalis*. The second possibility is that there has been introgression and/or incomplete lineage sorting of mtDNA variation across subspecies boundaries (sensu Klauber 1951). Although the available data do not allow us to distinguish these alternatives, both are likely at play. The first alternative (inadequate morphological taxonomy) seems to be the most likely explanation for the subspecies designations of *C. o. talpina* and *C. o. klauberi*. Individuals from both are dispersed in relatively shallow tip clades of *C. o. occipitalis* and *C. o. annulata*, respectively. Our NMS morphological results were complimentary, where *C. o. talpina* variation completely encompassed variation documented in *C. o. occipitalis*. Similarly, the variation among *C. o. klauberi* and *C. o. annulata* broadly overlapped along the axis that accounted for the majority of morphological variation. So for these two subspecies we lean towards a synonomy hypothesis. However, it is interesting that both *C. o. talpina* and *C. o. klauberi* are found at extreme northern and eastern portions (respectively) of *C. occipitalis'* range and both occur at relatively higher elevations than either *C. o. occipitalis* or *C. o. annulata*, respectively. In addition, the color pattern characteristics between these subspecies are similar (i.e., both exhibit secondary dark maculation across dorsal/lateral interspaces). Thus, it may be possible that localized environmental forces (e.g. elevation and temperature) at the limits of *C. occipitalis'* range are affecting convergent color patterns and that the population structure identified in this study (restricted gene flow) may be helping to drive these localized forces in a directional sense, creating locally adapted morphological phenotypes or ecomorphs (Klauber 1939; King and Lawson 1995; Leaché and Reeder 2002).

Introgression or incomplete lineage sorting seems to be the best explanation for discordance observed at the geographic interface between *C. o. occipitalis* and *C. o. annulata*. Populations in southeastern California (where the transition between Colorado and Mojave Deserts is less physiographically distinct) show geographical inconsistencies between our molecular results and traditional taxonomy in that the *C. o. occipitalis* phenotype is observed in samples from both major clades (subclades A, B, and E; Fig. 2). These patterns are consistent with an incomplete lineage sorting hypothesis and/or secondary contact, with ongoing gene flow, of formerly isolated subspecies groups. Interestingly, Klauber (1951) noted that eastern Mojave populations of *C. o. occipitalis* "show a tendency toward annulata" in having lower body band counts and a higher frequency of ventral markings. This same pattern was recovered in our Bayesian phylogram where *C. o. occipitalis* haplotypes from eastern Mojave (subclade E) were nested within the southeastern clade which largely consisted of *C. o. annulata* haplotypes. He also noted that populations of *C. o. occipitalis* "most widely differentiated from *C. o. annulata*" inhabit the extreme western part of the Mojave Desert, a pattern concordant with our northwestern clade. The consistency of these morphological patterns with our mtDNA analyses provides some basis for the continued recognition of these subspecies units. So in a general sense *Chionactis occipitalis* found in the northwestern clade possess more brown primary dorsal crossbands and no red secondary bands; while southeastern clade *C. occipitalis* have fewer black dorsal crossbands and possess secondary red bands (in addition to the morphological differences detected in this study). Nonetheless, we would encourage further hypothesis testing using increased genetic sample sizes and nuclear DNA data to help resolve these alternatives.

Conservation

Correct characterization of groupings below the species level (i.e., subspecies, population segments, ESUs) is essential to conservation efforts. The prominent idea to prioritizing units for protection has been the concept of the evolutionary significant unit (ESU; Ryder 1986). However, the nature and criteria used to delineate ESUs has been increasingly controversial, and recent discussions have even challenged the dichotomous nature inherent in designating ESUs given the continuum through which populations evolve (Crandall et al. 2000; Goldstein et al. 2000; Fraser and Bernatchez 2001; Holycross and Douglas 2007). Therefore, in taking the first steps to characterize units of conservation within *C. occipitalis*, we focus on identifying population segments that show evidence of

long-term evolutionary history based on our genetic data. Although our genetic and morphological analyses do not support recognizing the current subspecies designations as naturally defined ESUs, they do reveal significant genetic diversity and structure across the species range. Our phylogenetic analyses presented herein demonstrate genetic isolation and independent evolutionary trajectories for the two primary clades (Northwestern and Southeastern; Fig. 2). Moreover, our landscape genetic analyses identified environmental differences and elevation barriers between the two clades which suggest that each persists under different ecological conditions. So at the deepest phylogenetic level our results (using both mtDNA and ecological evidence) potentially support the recognition of at least two distinguishable 'ESUs' or 'populations' following criteria given in Moritz (1994), Crandall et al (2000), and Fraser and Bernatchez (2001). However, it may be argued that up to 6 distinguishable units (subclades A-F; Fig. 2) may potentially be recognized, depending on the threshold level and criteria used to define ESU status. Alternatively, we posit that each of these subclades would better comprise 'management units" (MUs) within the more inclusive ESUs (i.e. the two primary clades). The subclades exhibit significant divergence for mitochondrial DNA required for MU status (Moritz 1994), and would thus represent the units at which population monitoring and demographic study is carried out within each ESU (sensu Moritz 1994). Nonetheless, the two main clades only partially fulfill Moritz's (1994) strict criteria, since both reciprocal monophyly at mtDNA alleles *and* significant divergence of allele frequencies at nuclear loci are required. In light of this fact, we recommend that these ESU hypotheses be further tested to investigate the extent of evolutionary isolation (with nuclear loci) and possible ecological/adaptive differences within *C. occipitalis*.

Recent arguments support continued recognition of subspecies under the ESA as long as these designations meet the "discreteness" and "significance" criteria of conservation units defined under the ESA (Haig et al. 2006). In regard to *C. o. klauberi*, our mtDNA sequence data and the available morphological data do not support the treatment of collection locations east and west of the purported morphological intergradation zone as "discrete" units for conservation and management purposes. Klauber (1951) discussed intergradation between *C. o. annulata* and *C. o. klauberi* extensively and considered its occurrence "unquestionable"; however, it is important to note that such assertions were not based on explicit analyses of data. Although the term "intergradation" was popular among mid 20th century taxonomists, a clear and explicit definition was never widely adopted. Furthermore, at the time there were no analytical techniques readily available to objectively evaluate its occurrence. In some instances intergradation seems to have been equated with hybridization between discrete taxonomic entities. In other contexts, intergradation appears to have been viewed as clinal variation where the intergrade represents an intermediate phenotype. Although our morphological data were consistent with the claim of intergradation (= clinal variation), they were not directly amenable to evaluating intergradation between *C. o. annulata* and *C. o. klauberi* either, since there were geographic gaps in sampling across the putative intergradation zone. Based on the collective consideration of our morphological results, the accumulation of past knowledge, and our mtDNA sequence data, we contend that *C. o. klauberi* represents a morphological endpoint of clinal variation without concordant phylogenetic distinction. Additionally, our NCPA suggested contiguous range expansion for snakes across central Arizona, indicating that gene flow is ongoing or has been until very recently between these putative subspecies pairs. If we employ the criteria of Moritz (1994), the "subspecies" *C. o. klauberi* would not qualify as an ESU due to the lack of reciprocal monophyly/exclusivity. In fact, there was no clear phylogenetic evidence that this group was on a separate evolutionary trajectory (see Fig 3a). Moreover, since the haplotypic variation exhibited in *C. o. klauberi* is largely shared with individuals identified as *C. o. annulata* (i.e. subclade F; Fig. 2), it does not even merit status as an MU. Using the less stringent criteria for ESU designation of Crandall et al. (2000), this group might show, at most, recent genetic inexchangeability due to anthropogenic effects (e.g. habitat fragmentation and loss). As such, it would fall under Case 8 with a management recommendation to treat subclade F (*C. o. annulata* + *C. o. klauberi*) as a single population and "restore [population structure] to historical condition" (Crandall et al. 2000). It is clear from our mtDNA data that in most cases, geographically proximate populations are more genetically similar to each other than to more distant populations, some even sharing the same haplotypes. Therefore, if translocations are proposed for reintroduction of *C. occipitalis* where populations have declined dramatically (e.g. Avra Valley populations in Arizona), then we would recommend harvesting from the most geographically proximate populations, although we would emphasize the need for further investigation and restoration of the habitat prior to undertaking interpopulation translocations (Dodd and Seigel 1991).

Our data also allow preliminary insight into the geographical structure of genetic variation of *C. occipitalis* across the Imperial/Coachella Valley, a region which retains considerable genetic diversity. This geographic region consists of low-elevation valleys and playas, surrounded by mesas consisting of sand dunes. However, recent human activities have greatly impacted this region. The valley is primarily inhabited by snakes from the

southeastern clade (subclade D); however, some of the northwestern clade haplotypes (subclade A) are represented in the northern portion of the Coachella Valley. These populations have likely dispersed southward along the Morongo Valley, which cuts north-south along the Transverse Ranges and empties into the Coachella Valley. A multiple species conservation plan (Coachella Valley Multiple Species Habitat Conservation Plan, MSHCP, 2006) has been developed for the entire Coachella Valley and surrounding mountains; however, management practices of covered species are largely based on conserving ecological processes of aeolian sand dune systems, with priority given to active dune versus stabilized dune systems. Therefore, if *C. occipitalis* habitat overlaps with that of species covered by the MSHCP then the genetic diversity represented in this region will likely be protected under the conservation plan. However, if *C. occipitalis* is more likely associated with stabilized dune systems then further protection may be required, especially in the northern portion of the valley, or this cryptic diversity will be lost.

Acknowledgements The Arizona Game and Fish Department (AGFD) provided funding that directly supported this project. Funding for tissue collections was received by USGS from Bureau of Land Management, Bureau of Recreation. We thank Bill Burger and Tom Jones for their field collection efforts and coordination of the volunteer collection efforts in Arizona. For contributing specimens and sharing information, data, and/or tissue samples we thank Randy Babb, Michael Barker, Kit Bezy, Robert Bezy, Valerie Boyarski, Thomas Brennan, Lisa Bucci, Kerry Crowther, Paul Daniel, Melanie Engstrom, Steve Goodman, Brad Hollingsworth, Larry Jones, Dominic Lanutti, Christine LiWanPo, Elizabeth Main, John Malone, Dan Mulcahy, Richard Myers, Lin Piest, Justin Pullins, Tanzy Pullins, Jim Rorabaugh, Phil Rosen, Angela Schwediman, Kirk Setser, Tim Snow, Donovan Wagner, Richard Wiggins, and the following institutions: San Diego Natural History Museum, Arizona State University. Collection was authorized by AGFD (SP613877, SP802036, SP572402), California Fish and Game Department (803038–04, 801135–04), and National Park Service (JOTR 25A0 9–07, JOTR-2005-SCI-0024). The use of trade, product, or firm names in this publication does not imply endorsement by the U.S. Government.

Appendix 1 Haplotype number, clade affiliation, collection locality, tissue number, and GenBank accession for each sample of *Chionactis occipitalis* used in the molecular portion of this study. Subspecies were assigned using a dichotomous key (Klauber 1951). However, if vouchers were not available subspecies assignment was based on geographic location (indicated by an asterisk).

Hap #	Clade	Collection location	Subspecies	Tissue #	Genbank #
1	Southeastern	Arizona: Maricopa, 8.0 mi (by road) E Mobile	intergrade*	B−6750	EU280331
2	Southeastern	Arizona: Pinal, Val Vista Rd, 1.3 mi W of Hwy 387, N of Casa Grande	annulata	ATH 714	EU280332
3	Southeastern	Arizona: Maricopa, Eagle Eye Rd, N of Salome Rd, 10 mi S of Aguila	annulata	ATH 708	EU280333
3	Southeastern	Arizona: Maricopa, 5.6 mi (by road) WSW Mobile	intergrade*	B−6660	EU280334
3	Southeastern	Arizona: Maricopa, 1.2 mi (by road) W Mobile	intergrade*	B−6738	EU280335
3	Southeastern	Arizona: Maricopa, 5.3 mi (by road) W Mobile	intergrade*	B−6752	EU280336
3	Southeastern	Arizona: Maricopa, 7.2 mi (by Hwy 238) WSW Mobile	intergrade*	B−6857	EU280337
3	Southeastern	Arizona: Maricopa, Hwy 238, 22.7 mi (by road) W of Hwy 347	intergrade*	TRJ 833	EU280338
3	Southeastern	Arizona: Maricopa, Hwy 238, 17.7 mi (by road) W jct Hwy 347	intergrade*	TRJ 839	EU280339
3	Southeastern	Arizona: Maricopa, Hwy 238, 1.5 mi (by road) E of Hwy 85 jct at Gila Bend	klauberi	TRJ 926	EU280340
4	Southeastern	Arizona: Pinal, Picacho Hwy, 0.2 mi S Nutt Rd, 0.8 mi N Harmon Rd	klauberi*	B−6981	EU280341
5	Southeastern	Arizona: Maricopa, Sun Valley Parkway, S of McDowell	annulata	ATH 713	EU280342
6	Southeastern	Arizona: Maricopa, Sun Valley Parkway, 9.9 mi N of I10	annulata	ATH 710	EU280343
7	Southeastern	Arizona: Maricopa, Eagle Eye Rd, 0.75 mi S of Pump Mine Wash	annulata	ASU 34684	EU280344
8	Southeastern	Arizona: Pinal, Hwy 79, 4.4 mi S of RR Xing	klauberi	ASU 34622	EU280345
8	Southeastern	Arizona: Pinal, Hwy 79, 1.4 mi S of RR Xing	klauberi	ASU 34623	EU280346
8	Southeastern	Arizona: Pinal, Florence	klauberi	RLB 6829	EU280347
9	Southeastern	Arizona: Pinal, Val Vista Rd, 1.7 mi NE of Maricopa - Casa Grande Hwy	annulata	ATH 715	EU280348
10	Southeastern	Arizona: Pinal, Casa Grande Hwy, 1.2 mi E of Val Vista Rd	annulata	ATH 717	EU280349
11	Southeastern	Arizona: Pinal, Casa Grande Hwy, 0.2 mi E of Montgomery Rd	klauberi	ATH 718	EU280350
12	Southeastern	Arizona: Pinal, West Phillips Rd, S of Hunt Hwy near the Santan Mountains	annulata	ATH 723	EU280351
12	Southeastern	Arizona: Pinal, Hwy 79, 5.3 mi S of Florence Jct	klauberi	TCB 182	EU280352

Appendix 1 continued

Hap #	Clade	Collection location	Subspecies	Tissue #	Genbank #
13	Southeastern	Arizona: Maricopa, Hwy 238 W of Mobile E of Maricopa Mtns	annulata	ATH 707	EU280353
14	Southeastern	Arizona: Pinal, ca 5.0 mi (by road) NNW Vaiva Vo; 0.1 mi N Tohono Boundary	klauberi*	B-6794	EU280354
15	Southeastern	Arizona: Pinal, Hwy 79: ca 6 mi S of Florence Jct	klauberi	ASU 35076	EU280355
16	Southeastern	Arizona: Pinal, Hwy 79, 9.4 mi S of Florence Jct	klauberi	TCB 181	EU280356
17	Southeastern	Arizona: Maricopa , Eagle Eye Rd, 0.3 mi S of Pump Mine Wash	annulata	ASU 34683	EU280357
18	Southeastern	Arizona: Pima, Hwy 85 S of Ajo	annulata	RDB 0074	EU280358
19	Southeastern	Arizona: Pinal, San Tan Mtns W Phillips Rd, S of Hunt Hwy	klauberi	ATH 709	EU280359
19	Southeastern	Arizona: Pinal, San Tan Mtns W Phillips Rd, S of Hunt Hwy	annulata	ATH 711	EU280360
19	Southeastern	Arizona: Pinal, San Tan Mtns intersection of Royce & Judd Rds	klauberi	ATH 716	EU280361
20	Southeastern	Arizona: Maricopa, Sun Valley Parkway, W of 219th Ave	annulata	ATH 712	EU280362
21	Southeastern	Arizona: Pinal, Hwy 79, 6.5 mi S of Florence Jct	klauberi	ASU 35071	EU280363
21	Southeastern	Arizona: Pinal, Hwy 79, 6.8 mi S of Florence Jct	klauberi	TCB 180	EU280364
22	Southeastern	Arizona: Maricopa, Eagle Eye Rd, N of Salome Rd	annulata	ATH 722	EU280365
23	Southeastern	Arizona: Maricopa, 16.1 mi (by road) WSW Mobile	intergrade*	B-6661	EU280366
24	Southeastern	Arizona: Maricopa, Hwy 238, 15.0 mi (by road) W jct AZ hwy 347	intergrade*	TRJ 840	EU280367
25	Southeastern	Arizona: Yuma, Mohawk Dunes	annulata	UTA R-54424	EU280368
26	Southeastern	Arizona: Yuma, Mohawk Dunes	annulata	UTA R-54425	EU280369
27	Southeastern	California: San Bernardino, Hwy 62 E of 29 Palms, near Sheep Hole Mtns	occipitalis	JMM 109	EU280370
28	Southeastern	California: Riverside, Joshua Tree	occipitalis	JOS 1106	EU280371
29	Southeastern	Arizona: Mohave, S of Yucca on I40 Frontage Rd, 6.6 mi S of Yucca	occipitalis	UAZ56456	EU280372
30	Southeastern	Arizona: Mohave, S of Yucca on I40 Frontage Rd, 7.2 mi S of Yucca	occipitalis	UAZ56455	EU280373
31	Southeastern	Arizona: Mohave, S of Yucca on I40 Frontage Rd, 7.4 mi S of Yucca	occipitalis	UAZ65457	EU280374
32	Southeastern	California: San Bernardino, Hwy 62, 32 mi W of Vidal Jct	occipitalis	CAS 223594	EU280375
33	Southeastern	California: Imperial, Algadones Dunes; ca 1/8 mi S of Ogilby exit off I-8	annulata	ASU 34682	EU280376
34	Southeastern	California: Imperial, Cargo Muchacho Mtns, Hwy 34, 1.1mi (by road) N of I-8	annulata	JMM 111	EU280377
35	Southeastern	California: Imperial, Ogilby Rd, 15.0 mi (by road) N of I-8	annulata	UTA R-51271	EU280378
36	Southeastern	California: Imperial, Hwy 78, 21.9 mi (by road) W jct Ogilby Rd	annulata	UTA R-51270	EU280379
37	Southeastern	Arizona: Yuma, Barry M Goldwater Airforce Base, 6 mi SE of 19th ST, Yuma AZ	annulata	JMM 1	EU280380
39	Southeastern	Arizona: Yuma, Barry M Goldwater Airforce Base, 6 mi SE of 19th ST, Yuma AZ	annulata	JMM 2	EU280381
38	Southeastern	Arizona: Yuma, Yuma Dunes, vicinity of County Rd 21 and Avenue A	annulata	ASU 35960	EU280382
40	Southeastern	California: San Diego, Hwy 78, 0.4 mi (by road) W jct Yaqui Pass Rd	annulata	UTA R-51277	EU280383
41	Southeastern	California: San Diego, Hwy 78, 0.7 rd mi E jct Borrego Springs Rd	annulata	KWS 49	EU280384
42	Southeastern	California: San Diego, Hwy 78, 1.6 rd mi E jct Borrego Springs Rd	annulata	KWS 39	EU280385
42	Southeastern	California: Imperial, Salton Sea Array 10	annulata	SASSP2–65	EU280386
43	Southeastern	California: Imperial, Salton Sea Array 12	annulata	SASSP3–8	EU280387
43	Southeastern	California: Imperial, Salton Sea Array 11	annulata	SASSP12–14	EU280388
44	Southeastern	California: San Diego, Borrego Springs Rd, 3.5 mi (by road) NW jct Hwy 78	annulata	KWS 53	EU280389

Appendix 1 continued

Hap #	Clade	Collection location	Subspecies	Tissue #	Genbank #
45	Southeastern	Arizona: Yuma, Hwy 95 S of Quartzite	annulata	ATH 719	EU280390
45	Southeastern	Arizona: Yuma, Hwy 95 S of Quartzite, 1.8 mi S of Palm Canyon Rd	annulata	ATH 720	EU280391
46	Southeastern	Arizona: La Paz, E of Parker on Shea Rd (Osborne Well Rd)	annulata*	ASU 35072	EU280392
47	Southeastern	Arizona: La Paz, Alamo Dam Rd, 30.8 mi N of Hwy 60, S of Alamo Lake	annulata	ATH 706	EU280393
48	Southeastern	Arizona: Yavapai, Hwy 71, 10.0 mi SW jct Hwy 93	annulata	TRJ 936	EU280394
49	Southeastern	Arizona: Yavapai, Hwy 71, 15.3 mi SW jct Hwy 93	annulata	TRJ 937	EU280395
50	Northwestern	California: Riverside, Mesa Array 10	occipitalis	MES 571	EU280396
50	Northwestern	California: Riverside, Mesa Array 3	occipitalis	MES 295	EU280397
51	Northwestern	California: Riverside, Palm Canyon	occipitalis	CJH3–127–86	EU280398
52	Northwestern	California: San Bernardino, Twentynine Palms, outside of	occipitalis	BLM 179	EU280399
52	Northwestern	California: San Bernardino, Marine Corp Air Command Center, Twentynine Palms	occipitalis	MCC 385	EU280400
52	Northwestern	California: San Bernardino, Marine Corp Air Command Center, Twentynine Palms	occipitalis	MCC 209	EU280401
53	Northwestern	California: Kern, Dove Springs	occipitalis	SDS 72189	EU280402
54	Northwestern	California: Kern, Dove Springs	occipitalis	SDS 72192	EU280403
55	Northwestern	California: Inyo, Hwy 127, 12.4mi S of Death Valley jct	talpina	JMM 62	EU280404
56	Northwestern	California: San Bernardino, Dumont Dunes, Hwy 127	occipitalis	CSB3–56–1	EU280405
57	Northwestern	California: Inyo, Panamint Valley Rd, 7.2mi S of jct Hwy 190	talpina	JMM 113	EU280406
57	Northwestern	California: Inyo, Panamint Valley Rd, 7.2mi S of jct Hwy 190	talpina	JMM 114	EU280407
57	Northwestern	California: Inyo, 12.6mi S jct Hwy 190 on Panamint Valley Rd	talpina	JMM 78	EU280408
58	Northwestern	California: San Bernardino, Trona Rd, 8.3 mi S jct Hwy 178	occipitalis	JMM 80	EU280409
59	Northwestern	California: Kern, Dove Springs	occipitalis	SDS 72190	EU280410

Appendix 2 Morphological characters

1. Average number of loreal scales (LOR)
2. Average number of ventral scales (VENT)
3. Average number of subcaudal scales (CS)
4. Average number of mid-dorsal scales between the junction of the parietal scales and first body band (PTFB)
5. Average number of tail bands (TB)
6. Hemipenal muscle attachment level (in subcaudal scales) divided by total number of subcaudal scales (HEM)
7. Average number of primary dark dorsal body bands (BB)
8. Average number of unblotched band positions on the ventrum divided by the number of primary body bands (UBPB)
9. Ratio of the mean width of primary bands divided by mean width of interspaces between them (DL)
10. Ratio of orbit width divided by head length (OWHL)
11. Ratio of head length divided by snout-vent length (HLSVL)
12. Ratio of tail length divided by total length (TAILTO)
13. Frontal flare, or ratio of posterior width of frontal scale divided by anterior width (FRONFL)
14. Tangent of the angle that the leading edge of the frontal scale forms with the perpendicular (FRONTN)

References

Alfaro ME, Zoller S, Lutzoni F (2003) Bayes or bootstrap? A simulation study comparing the performance of Bayesian Markov chain Monte Carlo sampling and bootstrapping in assessing phylogenetic confidence. Mol Biol Evol 20:255–266

Anderson MJ (2004) DISTLM Version 5: a FORTRAN computer program to calculate a distance-based multivariate analysis for a linear model. Department of Statistics, University of Auckland, New Zealand. http://www.stat.auckland.ac.nz/~mja. Cited 16 Jun 2005

Avise JC (1994) Molecular markers, natural history and evolution. Chapman & Hall, New York

Avise JC (1996) Toward a regional conservation genetics perspective: phylogeography of faunas in the southeastern United States. In: Avise JC, Hamrick JL (eds) Conservation genetics: case histories from nature. Chapman and Hall, New York, pp 431–470

Ayoub NA, Riechert SE (2004) Molecular evidence for Pleistocene glacial cycles driving diversification of a North American desert spider, *Agelenopsis aperta*. Mol Ecol 13:3453–3465

Babik W, Branicki W, Crnobrnja-Isailovic J et al (2005) Phylogeography of the two European newt species-discordance between mtDNA and morphology. Mol Ecol 14: 2475–2491

Bailey RG, Avers PE, King T et al (eds) (1994) Ecoregions and subregions of the United States (map). Washington, DC, US

Geological Survey. Scale 1:7,500,000. Accompanied by a supplementary table of map unit descriptions, McNab WH, Bailey RG (eds). Prepared for the USDA, Forest Service
Bethancourt JL (2004) Arid lands paleobiogeography: the rodent midden record in the Americas. In: Lomolino MV, Heaney LR (eds) Frontiers in biogeography. Sinauer Associates, Sunderland MA, pp 27–65
Brandley MC, Schmitz A, Reeder TW (2005) Partitioned Bayesian analyses, partition choice, and phylogenetic relationships of scincid lizards. Syst Biol 54:373–390
Center for Biological Diversity (2004) Petition to list the Tucson Shovel-nosed snake (*Chionactis occipitalis klauberi*) as an endangered species. Available from http://www.biologicaldiversity.org/swcbd. Cited 15 Dec 2004
Clement M, Posada D, Crandall KA (2000) TCS: a computer program to estimate gene genealogies. Mol Ecol 9:1657–1659
Coachella valley multiple species habitat conservation plan (2006). Available from http://www.cvmshcp.org/prdplan/CVMSHCP_final.htm
Coyn JA, Orr HA (2004) Speciation. Sinauer Associates Inc., Boston
Crandall KA, Beninda-Emonds ORP, Mace GM et al (2000) Considering evolutionary processes in conservation biology. TREE 15:290–295
Cross JK (1979) Multivariate and univariate character geography in *Chionactis* (Reptilia: Serpentes). PhD Thesis, The University of Arizona
Dodd CK Jr, Seigel RA (1991) Relocation, repatriation, and translocation of amphibians and reptiles: Are they conservation strategies that work? Herpetologica 47:336–350
Douglas ME, Douglas MR, Schuett GW et al (2002) Phylogeography of the Western Rattlesnake (*Crotalus viridis*) complex, with emphasis on the Colorado Plateau. In: Shuett GW, Hoggren M, Douglas ME, Greene HW (eds) Biology of the Vipers. Eagle Mountain Publishing, LC, Eagle Mountain, UT, pp. 11–50
Douglas ME, Douglas MR, Schuett GW et al (2006) Evolution of rattlesnakes (Viperidae; *Crotalus*) in the warm deserts of western North America shaped by Neogene vicariance and Quaternary climate change. Mol Ecol 15:3353–3374
Excoffier L, Laval G, Schneider S (2005) Arlequin ver. 3.0: An integrated software package for population genetics data analysis. Evol Bioinform Online 1:47–50
Felsentein J (1985) Confidence limits on phylogenies: an approach using bootstrap. Evolution 39:783–791
Fraser DJ, Bernatchez L (2001) Adaptive evolutionary conservation: towards a unified concept for identifying conservation units. Mol Ecol 10:2741–2752
Funk DJ, Omland KE (2003) Species-level paraphyly and polyphyly: frequency, causes, and consequences, with insights from animal mitochondrial DNA. Annu Rev Ecol Syst 34:397–423
Gatesy J, Desalle R, Wheeler W (1993) Alignment-ambiguous nucleotide sites and the exclusion of systematic data. Mol Phylogenet Evol 2:152–157
Geffen E, Anderson MJ, Wayne RK (2004) Climate and habitat barriers to dispersal in the highly mobile grey wolf. Mol Ecol 13:2481–2490
Goldstein PZ, Desalle R, Amato G et al (2000) Conservation genetics at the species boundary. Conserv Biol 14:120–131
Haig SM, Beever EA, Chambers SM et al (2006) Taxonomic considerations in listing subspecies under the U.S. Endangered Species Act Conserv Biol 20:1584–1594
Hillis DM, Bull JJ (1993) An empirical test of bootstrapping as a method for assessing confidence in phylogenetic analysis. Syst Biol 42:182–192
Hillis DM, Mable BK, Larson A et al (1996) Nucleic acids IV: Sequencing and cloning, In: Hillis DM, Moritz C, Mable BK (eds) Molecular systematics, 2nd edn. Sinauer, Sunderland, Massachusetts, pp 231–381
Holycross AT, Douglas ME (2007) Geographic isolation, genetic divergence, and ecological non-exchangeability define ESUs in a threatened sky-island rattlesnake. Biol Conserv 134:142–154
Huelsenbeck JP, Ronquist F (2001) MRBAYES: Bayesian inferences of phylogenetic trees. Bioinform 17:754–755
Irwin DE (2002) Phylogeographic breaks without geographic barriers to gene flow. Evolution 56:2383–2394
Janzen FJ, Krenz JG, Haselkorn TS et al (2002) Molecular phylogeography of common garter snakes (*Thamnophis sirtalis*) in western North America: implications for regional historical forces. Mol Ecol 11:1739–1751
Jensen JL, Bohonak AJ, Kelley ST (2005) Isolation by distance, web service. BMC Genet 6:13
Kimura M (1980) A simple method of estimating evolutionary rates of base substitutions through comparative studies of nucleotide sequences. J Mol Evol 16:111–120
King RB, Lawson R (1995) Color-pattern variation in Lake Erie water snakes: the role of gene flow. Evolution 49:885–896
Klauber LM (1937) A new snake of the genus *Sonora* from Mexico. Trans San Diego Soc Nat Hist 8:363–366
Klauber LM (1939) Studies of reptile life in the arid southwest. Bull Zoo Soc San Diego 14:65–79
Klauber LM (1951) The shovel-nosed snake, *Chionactis* with descriptions of two new subspecies. Trans San Diego Soc Nat Hist 11:141–204
Leaché AD, Reeder TW (2002) Molecular Systematics of the eastern fence lizard (*Sceloporus undulatus*): a comparison of parsimony, likelihood, and bayesian approaches. Sys Biol 51:44–68
Legendre P, Anderson MJ (1999) Distance based redundancy analysis: testing multispecies responses in multifactorial ecological experiments. Ecol Monogr 69:1–24
Mahrdt CR, Beaman KR, Rosen PC et al (2001) *Chionactis occipitalis*. Catalog Am Amphib Reptile 731:1–12
McArdle BH, Anderson MJ (2001) Fitting multivariate models to community data: a comment on distance-based redundancy analysis. Ecology 82:290–297
McCune B, Mefford MJ (1999) PC-ORD: Multivariate analysis of ecological data version 4.26. MjM Software Design, Gleneden Beach, Oregon
Miller MP (2005) Alleles in space (AIS): Computer software for the joint analysis of interindividual spatial and genetic information. J Hered 96:722–724
Miller MP, Bellinger R, Forsman ED, Haig SM (2006) Effects of historical climate change, habitat connectivity, and vicariance on genetic structure and diversity across the range of the red tree vole (*Phenacomys longicaudus*) in the Pacific Northwestern United States. Mol Ecol 15:145–159
Mortiz C (1994) Applications of mitochondrial DNA analysis in conservation: A critical review. Mol Ecol 3:401–411
Murphy RW, Trépanier TL, Morafka DA (2007) Conservation genetics, evolution and distinct population segments of the Mojave fringe-toed lizard, *Uma scoparia*. J Arid Environ 67:226–247
Nylander JAA (2002) MrModeltest v1.0b. Program distributed by the author via http://www.abc.se/~nylander/. Cited 27 Apr 2007
Nylander JAA, Ronquist F, Huelsenbeck JP et al (2004) Bayesian phylogenetic analysis of combined data. Syst Biol 53:47–67
Osada N, Wu C (2005) Inferring mode of speciation from genomic data: a study of the Great Apes. Genetics 169:259–264
Pilot M, Jedrezejewski W, Branicki W et al (2006) Ecological factors influence population genetic structure of European grey wolves. Mol Ecol 15:4533–4553

Posada D, Crandall KA, Templeton AR (2000) GEODIS: a program for the cladistic nested analysis of the geographical distribution of genetic haplotypes. Mol Ecol 9:487–488

Rosen PC (2003) Avra Valley snakes: Marana survey report for Tucson Shovel-nosed snake (*Chionactis occipitalis klauberi*). Final Report on shovel-nosed snake prepared for Town of Marana. University of Arizona, Tucson, AZ

Ryder OA (1986) Species conservation and the dilemma of subspecies. TREE 1:9–10

Schulte II JA, Macey JR, Papenfuss TJ (2006) A genetic perspective on the geographic association of taxa among arid North American lizards of the *Sceloporus magister* complex (Squamata: Iguanidae: Phrynosomatinae). Mol Phylogenet Evol 39:873–880

Shaw KL (2002) Conflict between nuclear and mitochondrial DNA phylogenies of a recent species radiation: what mtDNA reveals and conceals about modes of speciation in Hawaiian crickets. Proc Natl Acad Sci USA 99:16122–16127

Stickel WH (1941) The subspecies of the Spade-nosed snake, *Sonora occipitalis*. Bull Chicago Acad Sci 6:135–140

Swofford DL (2002) *PAUP*: Phylogenetic Analysis Using Parsimony (* and Other Methods)*, Version 4.0b10. Sinauer, Sunderland, Massachusetts

Templeton AR (1998) Nested clade analyses of phylogeographic data: testing hypotheses about gene flow and population history. Mol Ecol 7:381–397

Templeton AR (2004) Statistical phylogeography: methods of evaluating and minimizing inference errors. Mol Ecol 13:789–809

Templeton AR, Crandall KA, Sing CF (1992) A cladistic analysis of phenotypic associations with haplotypes inferred from restriction endonuclease mapping and DNA sequence data. III. Cladogram estimation. Genetics 132:619–633

Thompson JD, Gibson TJ, Plewniak F et al (1997) The ClustalX windows interface: Flexible strategies for multiple sequence alignment aided by quality analysis tools. Nucleic Acids Res 24:4876–4882

Trépanier TL, Murphy RW (2001) The Coachella Valley Fringe-toed lizard *Uma inornata*: genetic diversity and phylogenetic relationships of an endangered species. Mol Phylogenet Evol 18:327–334

USFWS (U.S. Fish, Wildlife Service) and NMFS (National Marine Fisheries Service) (1996) Policy regarding the recognition of distinct vertebrate population segments under the Endangered Species Act. Fed Regist 61:4721–4725

Van Devender TM, Thompson RS, Betancourt JL (1987). Vegetation history of the deserts of southwestern North America; The nature and timing of the Late Wisconsin-Holocene transition. In: Ruddiman WF, Wright HE Jr (eds) North America and adjacent oceans during the last deglaciation. The Geology of North America K-3, Geological Society of America, Boulder, Colorado, pp 323–352

Wüster W, Yrausquin JL, Mijares-Urrutia (2001) A new species of indigo snake from north-western Venezuela (Serpentes: Colubridae: *Drymarchon*). Herpetol J 11:157–165